PYROLYSIS PARAMETERIZATION AND VALIDATION FOR POLYMERIC MATERIAL

Jing Li*[1,2] and Stanislav Stoliarov[1]
[1]Fire Protection Engineering, University of Maryland, College Park, Maryland, 20740
[2]Fire Science & Professional Studies, University of New Haven, West Haven, CT, 06516
*e-mail: jli@newhaven.edu

ABSTRACT

This work is focused on developing and applying a systematic methodology for the characterization of pyrolysis of polymeric materials based on milligram-scale and bench-scale tests to isolate a specific chemical and/or physical process in each scale level. The entire study is divided into two parts corresponding to two different scales of tests and analysis. The first part is concentrated on the measurement of kinetics and thermodynamics of the thermal degradation of polymeric materials at milligram-scale. It employs a simultaneous thermal analysis instrument capable of thermogravimetric analysis (TGA) and differential scanning calorimetry (DSC). All measured properties are incorporated into a continuum pyrolysis model. This model is subsequently employed to analyze DSC heat flow and extract sensible, melting and degradation reaction heats. The extracted set of kinetic and thermodynamic parameters is shown to simultaneously reproduce TGA and DSC curves. This procedure was used to characterize fifteen widely used commercial polymers.

The second part of this study was extended to bench-scale gasification experiments that were carried out using a controlled atmosphere calorimetric pyrolysis apparatus (CAPA), which has been recently developed in our group. The CAPA is used to measure material gravimetric and thermal changes during thermal decomposition in an anaerobic atmosphere with a capability of analyzing material thermal transport properties. These properties, combined with material kinetics and thermodynamics from the first part of this study, served as inputs for this fully parameterized model simulating one-dimensional pyrolysis under wide range of external heat fluxes. The predictive power of this model and validity of its parameters are verified against the results of mass loss measurements. Seven out of fifteen polymers were validated in bench-scale and the parameterized simulations showed reasonable agreement with experimental data under wide range of conditions.

INTRODUCTION

Polymers are ubiquitous in both high technology and routine household applications. An attractive combination of customizable mechanical properties, low weight, and easy processability makes them an irreplaceable attribute of the modern society. One of the main disadvantages associated with a widespread use of these materials is their inherent flammability (Cullis and Hirschler 1981). An important step towards flame resistant polymeric structures and design solutions is development of models that relate chemical and physical properties of these materials to their performance in various fire scenarios. A number of such models have recently been developed including Gpyro (Lautenberger and Fernandez-Pello 2009), solid phase model in the NIST Fire Dynamics Simulator (McGrattan, Hostikka et al. 2013) and ThermaKin (Stoliarov, Leventon et al. 2014). As an input, these models require properties that describe kinetics and thermodynamics of material thermal degradation and define condensed-phase heat transport. The fact that many of the newly synthetic polymer fundamental properties are frequently unknown, prevents us from using these models in fire safety applications.

Besides estimating these properties from the experiments with parameter optimization algorithms(Lautenberger, Rein et al. 2006) (Chaos, Khan et al. 2011) (ASTM(E2058-09) 2009), an alternate way to acquire these fundamental properties is measuring the individual parameters with separate experimental devices and as it was performed by a number of researchers (Christian, Jean-Louis et al. 1987; Steckler 1991; Staggs and Whiteley 1999; Nicolette VV 2004; Lautenberger C 2005; Stoliarov, Crowley et al. 2009; Stoliarov, Crowley et al. 2010).

The current procedure is based on milligram-scale and bench-scale approaches to isolate specific chemical and/or physical processes in each test so that each property can be systematically measured or calculated from the data analysis and interpretation. In milligram scale approach, Thermogravimetric analysis (TGA) and differential scanning calorimetry (DSC) are among the most frequently used techniques employed for the measurement of the core subset of these properties. The main advantage of these techniques is associated with the use of small material samples (3-10 mg) and relatively slow and steady heating rates (3-30 K min^{-1}). These heating conditions minimize the effects of heat and mass transport inside the sample on mass loss and heat flow, which makes it possible to exclude the transport from data analysis and interpretation.

For bench-scale approach, gasification experiments that were carried out on a controlled atmosphere calorimetric pyrolysis apparatus (CAPA) which has been recently developed in our group. The CAPA is used to measure material gravimetric and thermal changes during thermal decomposition in a controlled atmosphere with a capability of analyzing material thermal transport properties.

EXPERIMENTAL

Milligram-scale approach

A Netzsch F3 Jupiter STA was employed in this study. This apparatus combines a TGA instrument equipped with 1 µg-resolution microbalance and a heat flux DSC implemented using a Netzsch TGA-DSC sample carrier equipped with P-type thermocouples. An anaerobic environment was created inside the furnace by continuously purging it with nitrogen at a rate of 50 cm^3 min^{-1}. TGA and DSC experiments were conducted simultaneously using the following heating program. A sample was first heated to 313 K and maintained at this temperature for 25 minutes. Subsequently, the sample was heated to 1223 K (873 K for non-charring polymers) at a heating rate of 10 K min^{-1}. The mass and heat flow data were collected only during the second, linear heating phase of the test. The selection of the heating rate was based on a recent theoretical analysis (Lyon, Safronava et al. 2012) that indicated that using 10 K min^{-1} for <10 mg samples ensures a uniform temperature inside the sample even when the heat associated with decomposition processes is significant. Additional TGA experiments were performed at 30 K min^{-1}. These experiments were used to evaluate how well the mass loss kinetics model developed using 10 K min^{-1} data performs at higher heating rates. All thermal analysis experiments were performed using Platinum-Rhodium crucibles as shown in Figure 1.

Fig. 1 Platinum-Rhodium crucibles with lids and a polymer sample inside.

Seven thermal analysis experiments (simultaneous TGA and DSC) were performed on each polymer. Averaged mass and heat flow curves were computed and used in further analysis. Averaging of heat flow curves from multiple experiments was shown to significantly reduce random errors and enable measurement of heat capacity (Li and Stoliarov 2013). Multiple experiments also provided the data necessary for the calculation of uncertainties in the extracted properties. Additional DSC experiments were performed on char residue produced in the polymer thermal analysis experiments. These experiments were performed on 3-5 mg samples at 10 K min^{-1} and were repeated 3 times for char produced from each material. The char was compacted in the crucible prior to DSC to ensure a good thermal contact with crucible bottom.

Char samples produced in the thermal analysis experiments were further examined with a Hitachi S3400 scanning electron microscope. The imaging was performed using 3 and 10 kV electrons. The purpose of this exercise was to determine whether there exist significant differences in the microscale topology of chars produced from different polymers.

Bench-scale approach

The Controlled Atmosphere pyrolysis Apparatus (CAPA), which detailed description is given in the earlier publication (Semmes, Liu et al. 2014) was modified to make it possible to focus an infrared camera on the bottom sample surface. A schematic of the modified CAPA is shown in Figure 2. The sample was placed on a 0.03 mm thick sheet of aluminum foil supported by a 0.8 mm thick aluminum mesh. The aluminum foil and mesh were coated with a high emissivity ($\varepsilon \approx 0.95$) paint.

A gold-coated, flat mirror (0.97 reflectivity in 0.8-10 µm range) was mounted about 10 cm below the sample to provide optical access for an infrared camera. The camera, FLIR E40, was mounted outside of the CAPA and focused on the aluminum foil supporting the sample bottom. The temperature readings were taken through the spacing in the aluminum mesh, which covered about 20% of the bottom sample surface. The camera was set for the paint emissivity. This novel solution to measure the sample bottom temperature was aim to provide non-contact, spatially-resolved thermometry. The advantages of this solution combined with CAPA in polymer gasification experiments are the following. As mentioned in the early studies (Semmes, Liu et al. 2014), bottom temperature using thermocouples and mass loss rate are taken separately because of the sensitivity of the balance is greatly affectedly by the thermocouple wires. In the modified setup, this issue is solved because of using non-contact measurement by IR camera which reduced the number of bench-scale experiments by a factor two. In addition, since material gravimetric and thermal changes during gasification were recorded simultaneously, this type of experimental setup provides more reliable data because two types of measurements (temperature and mass) are synchronized in time from exactly same experiments.

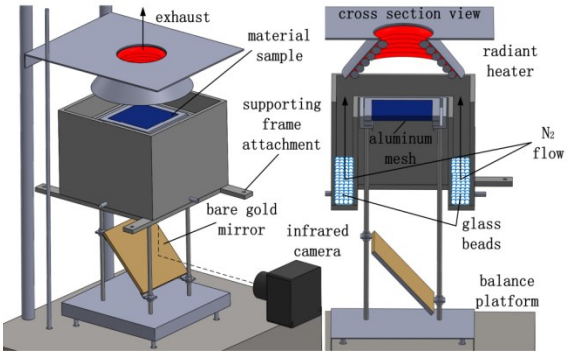

Fig. 2 Schematic of modified controlled atmosphere pyrolysis apparatus.

DATA ANALYSIS AND DISCUSSION

A numerical pyrolysis model, *ThermaKin* (Stoliarov, Leventon et al. 2014) , was used in this study to analyze TGA and DSC experiments and obtain a parametric description of the kinetics and thermodynamics of polymer degradation. *ThermaKin* solves mass and energy conservation equations describing zero-, one- or two-dimensional object subjected to external (convective and/or radiative) heat. The material of the object is represented by a mixture of components, which may interact chemically and physically. The components are assigned individual temperature-dependent properties and categorized as solids or gases.

The results of 10 K min^{-1} TGA experiments performed on PEEK are shown in Figure 3. The experimental mass loss rate (MLR) curve consists of one major peak followed by an extended shoulder. These features of MLR can be modeled by a sequence of two first order reactions:

PEEK $\rightarrow \theta_1$ PEEK_int,

PEEK_int $\rightarrow \theta_2$ PEEK_char,

where PEEK_int and PEEK_char denote condensed-phase decomposition products; and θ_1 and θ_2 are the corresponding product yields. Gas-phase products are not shown because they are assumed to leave the condensed phase and sample container instantaneously. Note that these reactions describe a semi-global decomposition mechanism formulated to capture key features of the polymer mass loss dynamics. Each reaction corresponds to tens or, perhaps, hundreds of elementary chemical processes occurring in the corresponding temperature range.

By adjusting Arrhenius parameters and product yields of these reactions in accordance with a procedure described elsewhere (Li and Stoliarov 2013), the reaction model was fit to the TGA mass loss. As shown in Figure 3, at 10 K min^{-1}, the model captures both mass and MLR behaviors accurately (R^2 = 0.95). Simulation of 30 K min^{-1} TGA experiments using the same reaction model yields poorer agreement (see Figure 3), which is likely to be caused by deviations of the experimental conditions from spatial isothermality assumed in the model.

Figure 4 shows the result of DSC experiments performed on PEEK. The heat flow normalized by the initial mass is plotted as a function of sample temperature. There are three distinct peaks in this curve. The lowest temperature peak is associated with melting. The higher temperature peaks approximately match the temperatures of the decomposition reactions.

At the first stage of analysis, the DSC curve was

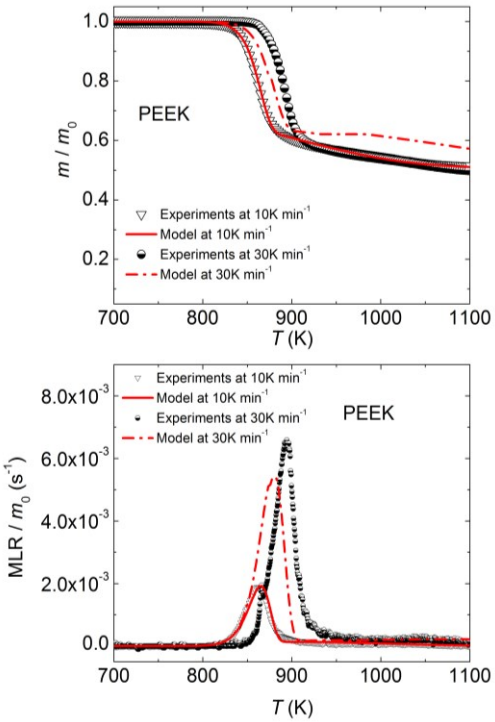

Fig. 3 Experimental and simulated TGA of PEEK at 10 and 30 K min^{-1}.

normalized by instantaneous heating rate and the regions of the curve not associated with melting or decomposition were fit with straight lines representing heat capacities of the solid and molten PEEK. PEEK_char heat capacity was obtained from separate experiments on the final decomposition residue.

The heat capacity of the intermediate component, PEEK_int, could not be resolved because of the overlap between the decomposition reactions. Therefore, the heat capacity of this component was assumed to be the mean of the heat capacity of molten PEEK and PEEK_char. The heat capacities weighted by a product of the corresponding compound mass of components and instantaneous heating rate were added to obtain a sensible heat flow baseline shown in Figure 4. The time evolution of the mass components was computed using *ThermaKin* from the TGA-derived reaction model.

Subtraction of this baseline from the total heat flow and subsequent integration of the difference in the melting region produced the value of the heat of melting (h_m). Integration of the difference in the decomposition region produced the value of the total heat of decomposition, which was subsequently divided between the first (h_1) and second (h_2) reactions. It should be noted that what is referred to here as the heat of decomposition reaction is actually a sum of heats of two processes: chemical decomposition process, which involves braking and formation of covalent chemical bonds and vaporization of the decomposition products, which involves braking of the Van der Waals bonds. Both of these processes change the system's enthalpy and cannot be separated within the framework of the current experiments.

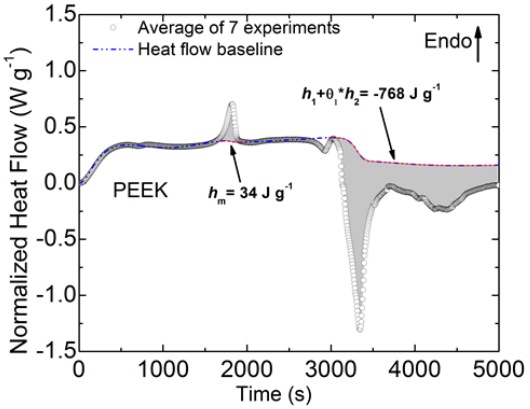

Fig. 4 Determination of decomposition reaction contributions to the PEEK DSC signal.

At the last stage of analysis, the thermodynamics of the parameterized reaction model was verified by comparing *ThermaKin* calculated heat flow with that observed in the experiments. This comparison is presented in figure 5 in a form of time resolved heat flow and heat flow integral. The experimental and simulated heat flow integrals match very well. The heat flow comparison is not as favorable. The discrepancies are thought to be due to the fact that the model assumes that the set heating rate (10 K min^{-1}) is always followed; while in the experiments, notable deviations from this heating rate are observed in the beginning and toward the end of the tests.

Perhaps, the most significant outcome of this analysis is an observation that PEEK, along with all other examined high char yield (>40 wt.%) polymers (Li and Stoliarov 2014), decomposes exothermically, while the rest of the polymers, including seven analyzed non-charring materials are characterized by an endothermic decomposition. Figure 6 provides SEM images of this residue, which appears to have relatively homogeneous, solid-like structure at micrometer scale. This structure is fundamentally different from that of intumescent polymer chars, which show a fractal-like void pattern with an extremely wide range of pore sizes (Staggs 2010).

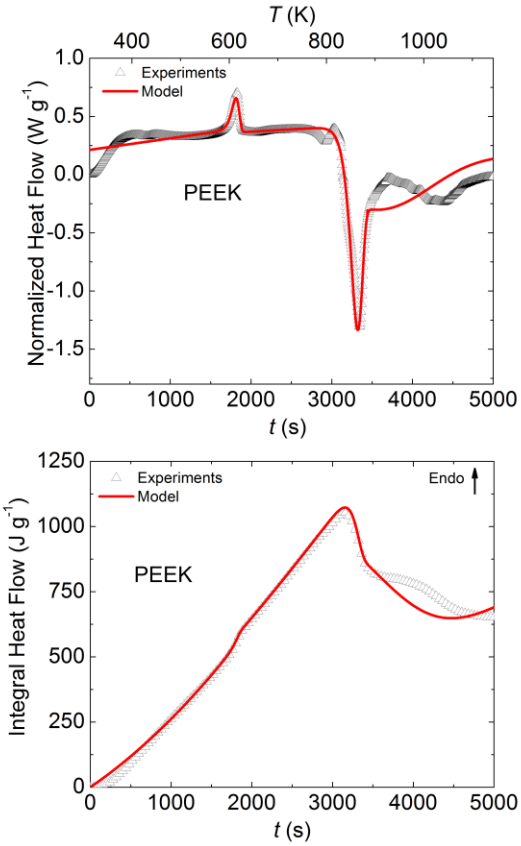

Fig. 5 Experimental and simulated DSC of PEEK at 10 K min^{-1}.

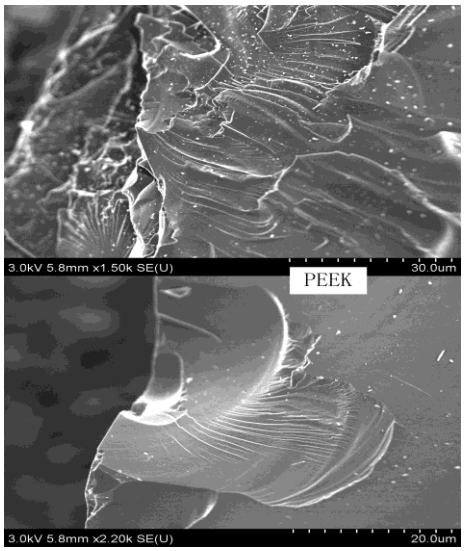

Fig. 6 SEM images of chars produced as a result of anaerobic thermal degradation of PEEK.

The relationship between the char yield and decomposition exothermicity can be explained by noting that a polymer char, which molecular structure is likely to be similar to that of graphite or soot (i.e.,

multiple fused aromatic rings), is highly thermodynamically stable. When this char is produced in sufficient amount, its thermodynamic stability compensates an increase in enthalpy associated with the formation of small molecular mass volatiles.

The temperature differences among the three areas of sample bottom surface can be investigated by displaying average temperature within each area for charring polymers, each area's sample bottom surface temperature is displayed individually, as an example shown in Figure 7 (circles) for ABS bottom surface temperature histories at 30 kW m^{-2}. The area 1 represents the sample surface center (4cm by 4cm) and areas 2-3 represent additional outer 1 cm strip. Each data point in Figure 7 for all the areas were calculated by averaging pixels over 3 gasification experiments and 36 pixels were randomly selected within corresponding area in each experiment.

In the bench-scale gasification experiments, IR camera was used to measure the temperature of the testing sample bottom surface. Since material thermal decomposition kinetics and thermodynamics are obtained, it is sufficient to run inverse modeling to obtain material thermal transport properties. The results of inverse modeling of this temperature are also presented in the Figure 7 (line). The thermal conductivities (k) for ABS and ABS char and absorption coefficient (α) for ABS char were adjusted (up to third order polynomial temperature-dependent function) to fit the bottom surface temperature. Please note that the densities of all the components for all the polymers in this study were not adjusted in the fitting. The thermal transport properties for all the components at condensed phase and their estimated uncertainties are reported in Table 1. The uncertainties were computed by propagating variation in the temperature measurements.

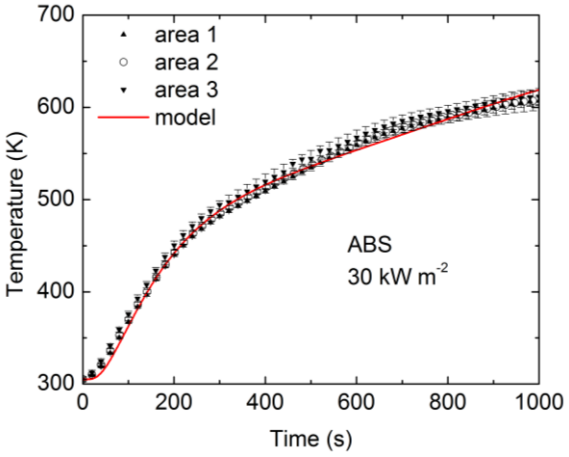

Fig. 7 Experimental and simulated bottom surface temperature histories obtained for ABS at 30 kW m^{-2}.

Table 1:Thermal transport properties for ABS.

Name	ρ (kg m^{-3})	ε	α (m^2 kg^{-1})	k (W m^{-1} K^{-1})
ABS	1050	0.95	1.71	$0.30\text{-}2.8\times10^{-4}T$
ABS_char	80	0.86	31.25	$0.13\text{-}5.4\times10^{-4}T$ $+4.8\times10^{-9}T^3$

As demonstrated in Figure 8 and Figure 9, the derived thermal conductivity parameters also provide a good description of 50 and 70 kW m^{-2} bottom surface temperature histories at a reasonable degree of accuracy. Those conditions were not used as optimization targets.

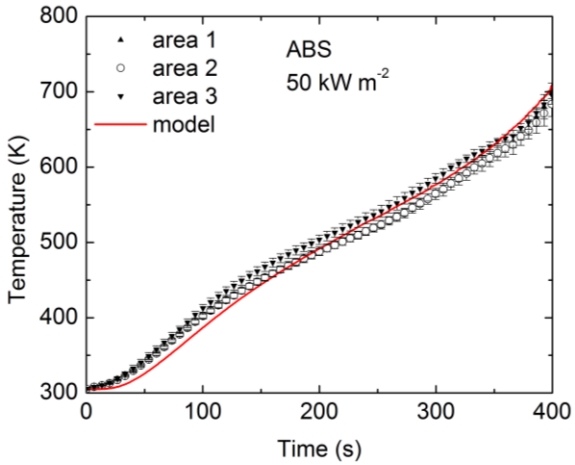

Fig. 8 Experimental and simulated bottom surface temperature histories obtained for ABS at 50 kW m^{-2}.

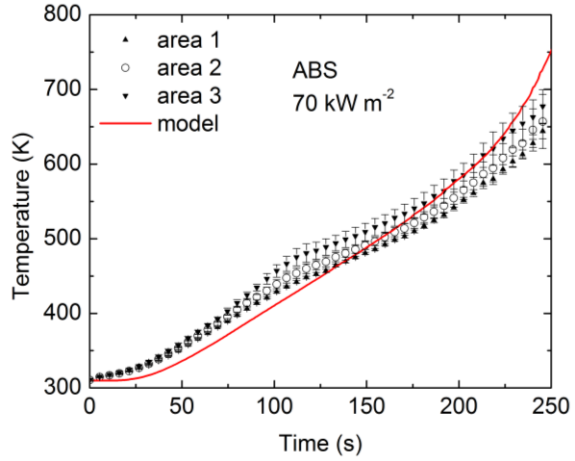

Fig. 9 Experimental and simulated bottom surface temperature histories obtained for ABS at 70 kW m^{-2}.

A comparison of the burning rates computed using the fully parameterized ABS model with the results of the gasification experiments is shown in Figure 10. The model predicts the burning rates with the accuracy comparable with the experimental repeatability except at 30 kW m^{-2}. Only at this heat flux level, ABS produced extremely larger amount of residues than it was measured in the TGA results. And this larger amount of residue forms thicker insulation layer on top of the virgin polymer and further affects the heat transfer inside the condensed

phase. The discrepancy is due to fact that thermal kinetic mechanism dose not represent the same pattern as obtained in the TGA test. Therefore, the model does not fully reflect the same amount of char residue in the ABS experiment. The effect of the char residues can be further demonstrated in the cases of external heat fluxes of 50 and 70 kW m^{-2}, when ABS samples are nearly completed degradation. The largest discrepancy between experiment results and model prediction is found to be about 20 % on average at 30 kW m^{-2} from beginning up to 800 s. And these average values for 50 and 70 kW m^{-2} are computed less than 10 % up to 400 s and 250 s respectively.

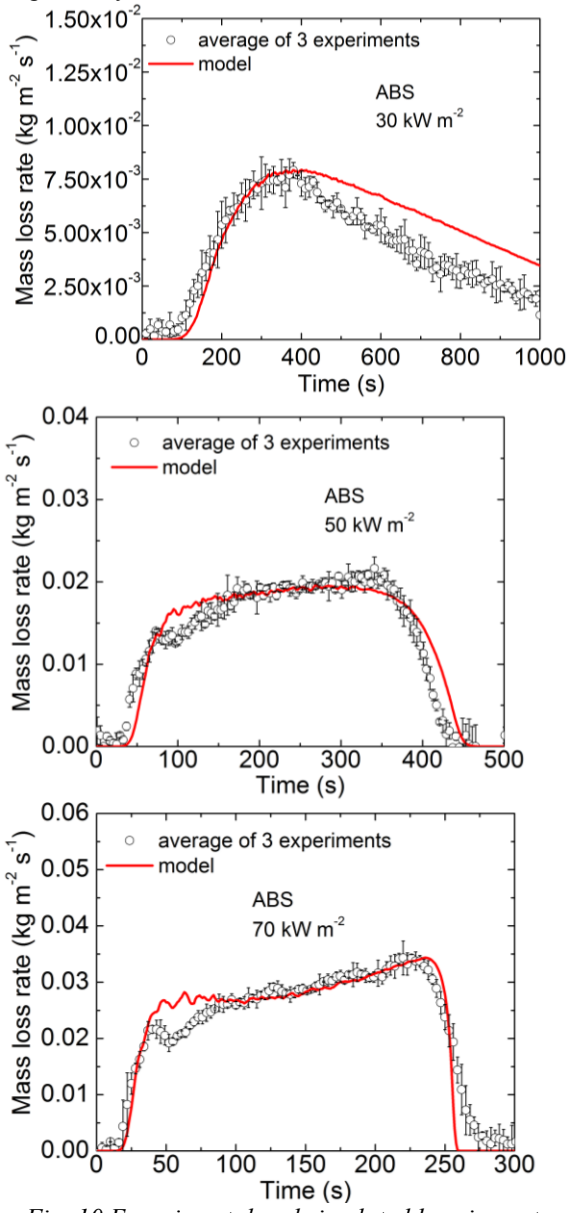

Fig. 10 Experimental and simulated burning rate histories obtained for ABS at 30-70 kW m^{-2}.

CONCLUSION:

This work was focused on developing and applying a systematic methodology for the characterization of pyrolysis of polymeric materials based on milligram-scale and bench-scale tests to isolate specific chemical and/or physical processes in each scale level. The main distinguishing feature of our approach is that experimental burning rate histories, which serve as the main target for optimization-based methods, are not utilized in the property calculation. Instead, they were employed to validate a fully parameterized model. This parameterization methodology minimizes possible compensation errors and extends the scope of the model validity. In essence, this combination of experiments and modeling represents a routine that generates complete property sets describing anaerobic pyrolysis of non-charring and charring polymers. The presented results clearly demonstrate that this routine produces consistent property values at a modest experimental cost.

REFERENCE

ASTM(E2058-09) (2009). Standard Test Methods for Measurement of Synthetic Polymer Material Flammability Using a Fire Propagation Apparatus (FPA). West Conshohocken, PA.

Chaos, M., M. M. Khan, et al. (2011). Evaluation of optimization schemes and determination of solid fuel properties for CFD fire models using bench-scale pyrolysis tests. Proc. Combust. Inst.

Christian, V., D. Jean-Louis, et al. (1987). "Experimental and Numerical Study of the Thermal Degradation of PMMA." Combustion Science and Technology 53(2-3): 187-201.

Cullis, C. F. and M. M. Hirschler (1981). The combustion of organic polymers. Oxford, New York, Clarendon Press, Oxford University Press.

Lautenberger C, F.-P. A. (2005). "Approximate Analytical Solutions for the Transient Mass Loss Rate and Piloted Ignition Time of a Radiatively Heated Solid in the High Heat Flux Limit." Fire Safety Science—Proceedings of the Eighth International Symposium, International Association for Fire Safety Science: 445-456.

Lautenberger, C. and C. Fernandez-Pello (2009). "Generalized pyrolysis model for combustible solids." Fire Safety Journal 44(6): 819-839.

Lautenberger, C., G. Rein, et al. (2006). "The application of a genetic algorithm to estimate material properties for fire

modeling from bench-scale fire test data." Fire Safety Journal 41(3): 204-214.
Li, J. and S. I. Stoliarov (2013). "Measurement of kinetics and thermodynamics of the thermal degradation for non-charring polymers." Combustion and Flame 160(7): 1287-1297.
Li, J. and S. I. Stoliarov (2014). "Measurement of kinetics and thermodynamics of the thermal degradation for charring polymers " Polymer Degradation and Stability 106: 2-15.
Lyon, R. E., N. Safronava, et al. (2012). "Thermokinetic model of sample response in nonisothermal analysis." Thermochimica Acta 545(0): 82-89.
McGrattan, K., S. Hostikka, et al. (2013). Fire Dynamics Simulator (Version 6) Technical Reference Guide National Institute of Standards and Technology Special Publication. 1: Mathematical Model.
Nicolette VV, E. K., Vembe BE. (2004). Numerical simulation of decomposition and combustion of organic materials. Proceedings of Interflam 10th International Conference on Fire Science and Engineering., Interscience Communications Ltd.: London.
Semmes, M., X. Liu, et al. (2014). A Model for Oxidative Pyrolysis for Corrugated Cardboard. Proceedings of the Eleventh International Symposium on Fire Safety Science (accepted for publication), University of Canterbury, New Zealand.
Staggs, J. E. J. (2010). "Thermal conductivity estimates of intumescent chars by direct numerical simulation." Fire Safety Journal 45(4): 228-237.
Staggs, J. E. J. and R. H. Whiteley (1999). "Modelling the combustion of solid-phase fuels in cone calorimeter experiments." Fire and Materials 23(2): 63-69.
Steckler, K. D., Kashiwagi, T., Baum, H.R. and Kanemaru, K. (1991). "Analytical Model For Transient Gasification Of Noncharring Thermoplastic Materials." Fire Safety Science 3: 895-904.
Stoliarov, S. I., S. Crowley, et al. (2009). "Prediction of the burning rates of non-charring polymers." Combustion and Flame 156(5): 1068-1083.
Stoliarov, S. I., S. Crowley, et al. (2010). "Prediction of the burning rates of charring polymers." Combustion and Flame 157(11): 2024-2034.
Stoliarov, S. I., I. T. Leventon, et al. (2014). "Two-dimensional model of burning for pyrolyzable solids." Fire and Materials 38(3): 391-408.